N O T I C E

THIS DOCUMENT HAS BEEN REPRODUCED FROM
MICROFICHE. ALTHOUGH IT IS RECOGNIZED THAT
CERTAIN PORTIONS ARE ILLEGIBLE, IT IS BEING RELEASED
IN THE INTEREST OF MAKING AVAILABLE AS MUCH
INFORMATION AS POSSIBLE

Combustion System Processes Leading to Corrosive Deposits

Carl A. Stearns and Fred J. Kohl
National Aeronautics and Space Administration
Lewis Research Center

and

Daniel E. Rosner
High Temperature Chemical Reaction Engineering Laboratory
Yale University

Combustion System Processes Leading to Corrosive Deposits

Carl A. Stearns and Fred J. Kohl
National Aeronautics and Space Administration
Lewis Research Center
Cleveland, Ohio 44135

and

Daniel E. Rosner
High Temperature Chemical Reaction Engineering Laboratory
Yale University
New Haven, Connecticut 06520

COMBUSTION SYSTEM PROCESSES LEADING TO CORROSIVE DEPOSITS*

Carl A. Stearns and Fred J. Kohl

National Aeronautics and Space Administration
Lewis Research Center
Cleveland, Ohio 44135

and

Daniel E. Rosner

High Temperature Chemical Reaction Engineering Laboratory
Yale University, New Haven, Connecticut 06520

ABSTRACT

Degradation of turbine engine hot gas path components by high tempera-
ture corrosion can usually be associated with deposits even though other
factors may also play a significant role. The origins of the corrosive
deposits are traceable to chemical reactions which take place during the
combustion process. In the case of hot corrosion/sulfidation, sodium sul-
fate has been established as the deposited corrosive agent even when none of
this salt enters the engine directly. The sodium sulfate is formed during
the combustion and deposition processes from compounds of sulfur contained
in the fuel as low level impurities and sodium compounds, such as sodium
chloride, ingested with intake air. In other turbine engine and power gen-
eration situations, corrosive and/or fouling deposits can result from such
metals as potassium, iron, calcium, vanadium, magnesium, and silicon.

Control strategies used to combat high temperature corrosion and fouling
problems can be aided by improved understanding of the thermochemistry,
kinetics, and dynamics of salt formation and deposition in the context of
combustion system processes. The chemistry of sulfur and various metal
salts in flame systems has been experimentally investigated. The flame
chemistry has been related to deposition processes and corrosion. Deposi-
tion mechanisms have been studied, and deposition measurements have been
made for a variety of systems. Deposition rate theories have been developed
and evaluated. The theories have evolved from the simple transport of a
single condensible vapor species to more general and accurate ones which
include multicomponent vapor transport, thermal diffusion, variable gas
properties across boundary layers, free stream turbulence, and particle size
effects.

This paper will present the current state of understanding of combustion
system processes leading to corrosive deposits by reviewing and summarizing
past and recent work on pertinent flame chemistry and deposition rate theory.

E-744

INTRODUCTION

Boilers, combustion turbine engines, and other types of directly fired energy conversion systems require components that will function properly, for long times, in hostile environments, at high temperatures and stresses (Refs. 1 and 2). Generally the components for such systems have been designed primarily on the basis of mechanical properties. In practice, however, hot section component life is found increasingly often to be controlled by environmental attack (Refs. 3 and 4). The attack derives from synergistic combinations of (1) the high temperatures involved, (2) the combustion products of the air and fuel burned, and (3) certain impurities which enter the system with the fuel and air. In the future, environmental attack problems can be expected to intensify because, as a consequence of the energy scenario, the operational trend is directed toward seeking high efficiency, brought about by the use of higher temperatures and pressures, while burning fuels with increased impurity content (Refs. 1 and 2).

Impurities are a key factor in life-controlling environmental attack of components. For fuels with essentially no impurities (e.g., natural gas), attack is usually manifested as only simple oxidation which is seldom life-limiting for modern superalloy coating materials (Refs. 5-12). However, certain impurities that enter the system can produce very accelerated, and often catastrophic, attack which can be life-limiting (Refs. 13-17). Sodium, potassium, vanadium and sulfur have been identified as particularily offensive (Refs. 13, 14, 16, 18, and 19), but other metals can also contribute to environmental attack under certain conditions (Refs. 15, 16, and 20). Attack can be manifested as material degradation and/or fouling of aerodynamic or heat transfer surfaces by the buildup of deposited substances. Modes of degradation include various types of high temperature corrosion, erosion and combined erosion-corrosion (Refs. 21 and 22). Except for erosion modes (consideration of which is outside the scope of this paper), accelerated attack beyond pure oxidation is usually associated, at least in part, with some sort of deposit of material on the surface. For the high temperature corrosion associated mainly with surface deposits of so-called corrosive agents, the attack might be hot corrosion (Refs. 23-31) or fireside corrosion (Refs. 32-35). For surface deposits which are corrosively benign, the attack might be fouling (Refs. 14, and 35-38). Obviously, the nature of the deposit and the rate of deposition are of primary importance in consideration of environmental attack. This paper addresses these two fundamental aspects of the environmental attack problem. Specifically considered are (1) the combustion chemistry of some inorganic impurities found in fossil fuel fired systems, and (2) the mechanisms and laws of deposition on surfaces exposed to the combustion product effluent flow from these systems.

COMBUSTION CHEMISTRY

From the point of view of environmental attack, it is essential to know the history and ultimate fate of impurities that enter the combustion system. The history aspect involves the combustion chemistry which, for most fossil fuel fired systems, is not well characterized. This situation can be attributed to two main factors: (1) there is a wide range in the number, type, and quantities of impurities involved; and (2) it is an exceedingly difficult task to make all of the necessary in situ composition, tempera-

ture, and kinetic measurements. Usually the combustion chemistry is inferred from characterizations of the deposits collected on probes placed in the particular combustion system in question (Refs. 13-15, 35, and 39-44); direct flame sampling/monitoring of all species in such systems is still lacking. Simple flame systems, such as H_2/O_2, CH_4/O_2, CH_4/air, etc. in laboratory contexts, have been studied extensively and the chemistry, while certainly not simple, is generally well in hand (Refs. 45-47). Laboratory flames seeded with various metal salts and inorganic compounds have also received considerable attention so that understanding in this area is developing (Refs. 47-49). However, almost no effort has been given to studying specific seeding compositions relevant to environmental attack and high temperature corrosion in particular. Only in the case of sulfur in combustion systems is there a large background of information and a reasonably complete understanding of the oxidation and combustion chemistry (Refs. 50-55).

Sulfate formation in flames. - Because sodium and potassium sulfates play such an important role in environmental attack, it is of considerable importance to know, especially in considering mechanisms of deposition, how and when sodium-sulfur-oxygen interactions occur. The works of Fenimore (Ref. 56) and Durie, et al. (Ref. 57) were attempts to determine the gas phase reactions of sodium species with sulfur in flames; from these works indirect evidence was obtained to suggest that, indeed, sodium-sulfur-containing species were formed in short residence times. Those studies, and the equilibrium calculations that were a fundamental part of them, did not, however, include thermodynamic data for the Na_2SO_4 gas phase molecule.

In 1975, the existence of the $Na_2SO_4(g)$ molecule was established by high-temperature Knudsen effusion-mass spectrometry, and values for the thermodynamic properties were provided (Ref. 58). With this information available, better equilibrium composition calculations were possible; such calculations showed the sodium-containing gas phase species to be a complicated function of temperature or fuel/oxidant mass ratio for any particular combustion system (Ref. 58). However, the question of the actual gas phase composition still remained to be established. To address this question, Stearns, et al. (Refs. 59 and 60) used high pressure, free-jet sampling mass spectrometric techniques (Ref. 61) to characterize and directly identify species in alkali metal salt/sulfur-doped, atmospheric pressure, premixed, fuel-lean methane/oxygen flames. Sulfur was added to the fuel-oxidant gas mixture as either gaseous sulfur dioxide or methyl mercaptan. The alkali salts were added by nebulizing aspirated aqueous solutions of the salt into the gas mixing chamber of the laminar flow, flat flame burner. Typical results obtained for a flame doped with sulfur dioxide and seeded with a sodium chloride water solution are presented in Fig. 1. The most significant points to be noted from the measured composition profiles are (1) the gaseous sodium sulfate molecule was observed to be formed in the flame, (2) this molecule was formed in less than one millisecond from the time when the reactants entered the flame, (3) gaseous sodium chloride and other sodium-containing gas phase species persist in the flame, (4) two intermediate species, $NaSO_2(g)$ and $NaSO_3(g)$, were directly identified in the flame, and (5) other gaseous combustion products (e.g., CO_2, H_2O, HCl, etc.) were identified in the flame. Not all species identified are shown in Fig. 1 because experimental considerations precluded profiling all species observed. The species $NaSO_2(g)$ and $NaSO_3(g)$ are not considered to be fragments because they were not observed as such in the Knudsen effusion vaporization of sodium sulfate (Ref. 58).

3

The next step was to make a comparison of the experimental observations with equilibrium thermodynamic predictions for the experimental reactant composition. The equilibrium thermodynamic calculations were made with the NASA complex chemical equilibrium computer code (Ref. 62). In the calcula-- tions the convention was used that CH_4 and SO_2 were labeled fuel while O_2, H_2O, and NaCl were labeled oxidant. Calculated equilibrium composi- tions of the reacted flame gas products, at the adiabatic flame temperature, are presented in Fig. 2 where the compositions are plotted as a function of the fuel/oxidant mass ratio. For the calculations, the program considered over seventy gaseous and condensed phase species made up of C-H-O-S-Na-Cl combinations, including $Na_2SO_4(g)$, but not $NaSO_2(g)$ or $NaSO_3(g)$ for which no thermodynamic data are available. The results of the calculations for the lean flames show that sodium is distributed in a complex pattern between $Na_2SO_4(c)$,* $NaOH(g)$, $Na_2SO_4(g)$, $Na(g)$, $NaCl(g)$, $(NaCl)_2(g)$, $NaO(g)$, and $NaH(g)$. At low values of the fuel/oxidant mass ratio, and up to a relatively abrupt cut-off, the sodium is tied up almost exclusively as the condensed phase Na_2SO_4. The gaseous species Na_2SO_4 is expected to be present in significant amounts only over a relatively narrow fuel/oxidant ratio range. Also, $Na_2SO_4(g)$ would always be expected to be present at a molar concentration of less than one- tenth that of $NaCl(g)$. At higher fuel/oxidant ratios, $NaOH(g)$, $Na(g)$, and $NaCl(g)$ are predicted to be the main carriers of sodium.

Experimental results are compared with the calculated equilibrium re- sults in Fig. 1. The calculated mole fraction column labeled 2032 (T_{adib}) is that calculated for the experimental flame conditions and an adiabatic flame temperature of 2032 K. These calculated compositions are seen to be in only fair agreement with the measured compositions. However, it must be recognized that for various reasons the true experimental flame temperature at the sampling orifice might be significantly different than the adiabatic flame temperature. Because the sampling probe and ambient conditions can conduct heat away from the flame, the experimental flame temperature would be expected in practice to be below the adiabatic temperature. Indeed this was found to be the case experimentally when the flame was probed with a simple thermocouple arrangement (Refs. 60 and 63). The thermocouple mea- surements indicated that the experimental flame was about 1832 K. There- fore, equilibrium compositions were calculated for this temperature and these compositions are also shown in Fig. 1.

Before making a final comparison between the measured and calculated compositions, a number of other important factors must be considered: (1) measured profiles as presented here have not been corrected for sampling and mass spectrometric sensitivity factors which are yet to be determined by "calibration" techniques (Ref. 63), and (2) the concentration level of sodium chloride in the flame has a considerable but unknown uncertainty associated with it because of the method used to introduced the sodium chlo- ride. Being cognizant of these considerations, we conclude that the agree- ment between experimental observations and calculated equilibrium composi- tions is reasonably good for all species. Furthermore, these results are taken to indicate that equilibrium calculations can be used with reasonable confidence to predict what species are to be expected and their relative levels.

---

*"c" represents a condensed phase, either solid or liquid.

Several other flame systems involving sodium, potassium, and sulfur have been studied by high pressure, free-jet expansion mass spectrometric techniques and some general results are listed in Table I. For each system, regardless of the form of the original sulfur or alkali metal salt, the appropriate alkali sulfate species was formed in the flame and the measured compositions were in good agreement with those calculated for equilibrium conditions.

Mechanisms of sodium sulfate formation. - The composition profiles shown in Fig. 1 for the species $NaSO_2(g)$, $NaSO_3(g)$, and $Na_2SO_4(g)$ bear on the kinetics and mechanism of formation of the $Na_2SO_4(g)$. As pointed out by Steinberg and Schofield (Ref. 64), NaOH, whether formed in one primary reaction or in two, appears to be a major potential precursor for the formation of sodium-sulfur compounds in flames. Fenimore (Ref. 56) favored $NaSO_2$ because for lean (and rich) H_2/air flames he found a decrease in the concentration of sodium atoms with the addition of large excesses of SO_2. In contrast, Durie, et al. (Ref. 57) found $NaSO_3$ formation more consistent with their lean flame observations. Only a few possibilities exist for homogenous gas phase formation of Na_2SO_4. Steinberg and Schofield consider the most probable one to be that involving a 2-body reaction and simple displacement, viz.,

$$NaOH(g) + NaSO_3(g) = Na_2SO_4(g) + H(g)$$
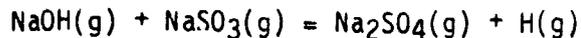
This is only speculation at this point in time but laser flourescence studies are currently in progress to elucidate the detailed mechanisms (Ref. 64).

Other combustion system sampling. - Greene, et al. have used high pressure, free-jet sampling mass spectrometric techniques in an attempt to directly sample and characterize the gaseous species responsible for fireside corrosion in fossil fuel fired systems (Refs. 65 and 66). Measurements were made on premixed gaseous flames and coal dust-air flames both seeded with potassium salts (e.g., KCl and K_2CO_3). The only potassium species definitely identified in preliminary studies were K and KOH; experimental complications precluded further characterization.

Wilson and Gillmore (Ref. 67) used a combination of techniques to study an alkali carbonate-seeded natural gas flame doped with sulfur dioxide. The combustion chamber simulated gas temperatures, velocities, and residence times of a large pulverized coal-fired boiler. While the gas characterization techniques were not strictly of the direct measurement type, they were a step beyond those inference techniques based on only an analysis of a collected deposit. Results obtained in this study establish that nearly equilibrium levels of alkali sulfates form in the flame zone dependent only on the physical mixing within the flame.

The preponderence of evidence appears to indicate that reactions responsible for the formation of alkali sulfates in combustion systems are sufficiently fast (1) to result in the formation of gas phase sulfate species, and (2) to allow the attainment of equilibrium compositions. Thus, it might then appear that the sulfate deposits observed to be responsible for corrosion and fouling are formed by the mere condensation of the respective gas species. However, deposition and mass transport investigations reveal that alkali sulfate gas may not be the only, or even the major, source contributing to deposition of the sulfate.

DEPOSITION

Deposition has long been recognized as an important aspect of environmental attack and numerous studies have been devoted to measuring deposition, characterizing deposits and elucidating deposition conditions (Refs. 13-17, 20, 31-39, 68-70, 72-74 and references cited therein). With the current revival of interest in the use of coal or coal-derived products and the increased impetus to utilize more impure liquid fuels, the deposition problem has taken on new emphasis. Insights into the techniques being employed and particular problems encountered can be gained by consultation of the cited references. However, detailed review of this entire area is beyond the objective of this paper.

Our consideration here shall be confined mainly to the ramifications of corrosive deposits and especially sodium sulfate. This is not to mitigate the role of other inorganic materials in high temperature corrosion or environmental attack. For example, the presence of iron, calcium, and phosphorous in fuels has been shown to lead to copious enough deposits to cause severe plugging of turbine-blade cooling holes (Ref. 36). Deposits containing lead compounds have been shown to be very corrosive (Ref. 20) as have those containing sodium-vanadium compounds (Ref. 18). In addition to the elements already noted, potentially harmful deposits could be formed from other elements and particularly those found in the mineral matter of various coals, e.g., silicon, aluminum, potassium, and magnesium (Ref. 14). Some very recent results obtained for coal-derived fuels (Ref. 43) and coal-oil mixtures (Ref. 44) have shown that the chemical compositions of the numerous deposits collected compared favorably with the predictions from equilibrium thermodynamic analyses. Furthermore, the substantial deposits observed in these studies resulted in insignificant corrosion and this was attributed to the fact that very little sodium or potassium sulfate was formed.

Deposition of sodium sulfate. - In 1965 Hedley et al. (Ref. 68) examined four possible mechanisms of deposition and outlined the applicable theories as they existed at that time. They concluded that particle diffusion probably plays no role in the overall deposition observed in practice while particle impaction could be the major mechanism operating for combustion systems with high gas velocities and large catchment surface areas. They felt that thermal diffusion could play a fairly important role for cooled surfaces but vapor diffusion was considered by them to be the predominant mechanism for cooled surfaces in low gas velocity flows. For vapor diffusion, the limiting temperature of the cooled surface for condensation was pointed out to be a function of gas stream concentration of components and the vapor pressure-temperature relationship for the particular ash content under consideration. This work was followed in 1966 by their experimental study of vanadium pentoxide deposition from a doped kerosene flame (Ref. 69). Hedley, et al. here demonstrated that, for their conditions, the dominant deposition mechanism was vapor diffusion and that their measured deposition rate results could be partially represented by the vapor diffusion rate equation they derived. Brown's later experimental study (Ref. 70) of the deposition of sodium sulfate was made as a function of air/fuel ratio, collector surface temperature, exposure time and so-called residence time, i.e., time from combustion plane to deposition collection surface. Brown used the same pilot scale, controlled mixing history furnace as used by Hedley, et al. (Ref. 69) and Brown showed that for this furnace, turbulence intensity was an important factor which should contribute to the deposition rate given by the Hedley, et al. vapor diffusion model. For

sodium sulfate the rate of deposition was found by Brown to be independent of excess air level, residence time and exposure time. The rate was, however, found to depend on collector surface temperature. The existence of a dew point was indicated and the dew point temperature was found to be a function of the sodium concentration added to the carbon disulfide-doped kerosene-fueled flame. Brown could not satisfactorily fit the rate-temperature curve to the vapor diffusion model, and he attributed the shape of the curve to droplet formation within the boundary layer.

The pioneering works of Hedley, Brown and Shuttleworth were followed by a deposition of sodium sulfate study conducted by Hanby (Ref. 40) who used a flame tunnel test rig. Based primarily on the fact that he found no sodium sulfate in his flames seeded with sodium chloride, Hanby concluded that in gas turbine engines the deposition process on turbine blades occurs by particle impaction. Hanby's results have recently been questioned (Ref. 71) because they are in apparent disagreement with more current findings (Refs. 59 and 60). An accurate analysis of Hanby's investigation is complicated by the nature of his experimental arrangement. Because of the way his dilution air was added, the exact fuel/air ratio in different sections of his combustor tunnel cannot be defined. Stearns, et al., would predict, from equilibrium calculations, that for Hanby's experiment with 5 percent excess air, no sodium sulfate should be expected to form; thus Hanby's results may not be contrary to current findings (Ref. 60).

Jackson (Ref. 72) used an air-cooled probe to study deposit formation in residual fuel oil-fired boilers. Mass transfer rates of ash constituents and magnesium compounds were measured at surface temperatures of 510° and 730° C. From measured rates of deposition and the analyzed deposit composition, both obtained in the absence of magnesium-containing additives, Jackson concluded that vapor diffusion of sodium hydroxide or sodium sulfate across the boundary layer is the dominant mode of deposition.

Urbas, et al. (Ref. 73) used a gas turbine combustor simulation rig, with actual first stage nozzle vane segments as collectors, to measure nozzle plugging rates as a function of (1) sodium concentration in the residual oil fuel and (2) firing temperature. They derived empirical expressions for plugging rate and developed a model which is independent of the number of high melting ash particles for constant levels of vanadium and magnesium. This would suggest a vapor diffusion mode.

Hart, et al. (Ref. 74) used a high pressure rig, modeled on a gas turbine, to study the effect of (1) fuel and air impurity levels, and (2) operation and combustion conditions on the amounts and chemistry of collected deposits. On the basis of their results, they concluded that deposition takes place by vapor diffusion accompanied by chemical change within the boundary layer at the surface collecting the deposit.

Recently Kohl, et al. (Ref. 75) used a high velocity (Mach 0.3) atmospheric pressure burner rig to study deposition from burning Jet A-1 fuel and air seeded with about 10 wppm of an inorganic salt (NaCl, sea salt or Na_2SO_4). Deposition on cylindrical platinum targets was studied as a function of target surface temperature. For each seeding salt the collected deposit was found to be mainly Na_2SO_4; only very minor amounts of other constituents were found for the sea salt tests. The existence of a dew point temperature was established and this condensation onset temperature was found to agree with that derived from equilibrium thermochemical calculations.

The experimental verification of a dew point temperature above which no deposition could be observed suggested that for the burner rig test condi-

tions, deposition was associated with vapor diffusion to the surface across a gaseous boundary layer. Accordingly, Rosner et al. (Refs. 76-82) have developed a convective diffusion theory, employing multicomponent vapor transport, for predicting deposition rates for sodium sulfate and other salts in burner rig experiments. Rosner's formulation is sufficiently general to include the transport of particles that are small enough to be treated as heavy molecules and that are dilute in the transfer gas flow mixture. Because this formulation represents current understanding, the theory shall be considered in some detail.

Vapor diffusion deposition rate theory. - If the combustion product gas temperature is sufficiently high to thermodynamically preclude the existence of condensed inorganic compounds, or if kinetic barriers prevent their appearance in the prevailing residence times, then condensates form only at surface temperatures below the dew point. The mechanism of mass transport to such surfaces is vapor diffusion across the combustion product flow boundary layers. Concentration (Fick), thermal (Soret) and turbulent diffusion contribute to the mass transport. If, on the other hand, the uncooled combustion product gas temperature is below the respective dew points for some offending species, condensates of these species may be present as an aerosol in the gas flow. Aerosols, either in the mainstream or formed within thermal boundary layers near cooler surfaces, influence deposition rates because (1) effective Fick and Soret diffusivities are altered from their purely vapor-values, and (2) sufficiently large size particles move differently than the local host gas mixture allowing them to cross gas streamlines and inertially impact surfaces. The important regimes of particle deposition are summarized in Table II where the smallest particles considered are the atoms and molecules of which vapors are composed. The size ranges specified are only approximate because it must be recognized that the mode is not fixed by particle size alone. The mode depends on the ratio of size to (1) the gas mean free path, (2) the characteristic viscous stopping distance, (3) the characteristic eddy scale, and (4) the collector dimensions.

To predict deposition rates quantitatively, it is convenient to neglect chemical reaction, condensation and/or coagulation within the thin mass transfer boundary layers adjacent to the surface. This is the tractable limiting case of a source-free (SF) or a "chemically frozen" boundary layer (BL) within which convection, turbulence, concentration (Fick or Brownian) diffusion and thermal (Soret) diffusion participate in mass transport to/from the surface. The multicomponent theory, sketched here, embraces all inorganic condensed phases and their vapor precursors, including mixtures and/or particles small enough to be considered heavy "molecules". Because the particles participating in the deposition process are often present in only trace amounts, for each such species or particle size class, i. present in local mass fraction ω_i, the diffusion mass flux law simplifies to:

$$\vec{j}_i'' = -D_i \rho (\nabla \omega_i + \alpha_i \omega_i \nabla \ln T) \quad (\omega_i \ll 1) \tag{1}$$

where ρ is density, T is temperature and $\vec{j}_i''$ is the flux vector. Here the two transport properties, D_i (Fick or Brownian diffusion coefficient) and α_i (dimensionless thermal diffusion factor), are specific to each species-host mixture combination. In the absence of mainstream turbulence and thermal diffusion, the form of Eq. (1) leads directly to the introduction of the dimensionless mass transfer coefficients $Nu_{m,i}$ (local

mass transport Nusselt numbers), defined such that each wall flux can be written:

$$-j''_{i,w}(SFBL, \alpha_i = 0) = \frac{(D_i \rho)_e}{L} \cdot Nu_{m,i}(x/L, Re, Sc_i, ...) \cdot (\omega_{i,e} - \omega_{i,w}) \quad (2)$$

Here the subscripts e and w respectively pertain to local conditions at the boundary layer outer and inner "edges" (Fig. 3), and Re and Sc_i are, respectively, the prevailing Reynolds' number based on characteristic length L and Schmidt number.

Insertion of thermal diffusion into the species or size class i mass conservation equation introduce₌ three effects:

(1) a convection-like (thermophoretic) transport term, producing a "suction like" augmentation of $Nu_{m,i}$;

(2) a "sink-like" term similar to that which would appear in the presence of homogeneous reaction of species or size class i;

(3) a non-Fick/Brownian diffusion contribution to the species or size class i flux at the wall (when $\omega_{i,w}$ is non zero).

Effects 1 and 2 on $Nu_{m,i}$ are lumped in the factor F_i (Soret) below which depends predominantly on the dimensionless thermophoretic "suction" parameter:

$$\tau_i = \alpha_{i,w}(Le_{i,w})^{1/3} [(T_e - T_w)/T_w] \quad (3)$$

However, F_i (Soret) is also influenced by the thermophoretic pseudo-sink operating both outside and inside the Brownian sublayer. Apart from turbulence within the boundary layer, mainstream turbulence (level and scale) can also augment transport rates to/from stationary surfaces. Thus, in practice, each mass transfer coefficient, $Nu_{m,i}$, must in addition be adjusted by a factor F_i (turb). Collecting these results, and in the absence of mainstream turbulence effects, each wall flux is then written as:

$$-j''_{i,w} = \frac{(D_i \rho)_e}{L} F_i(Soret)Nu_{m,i} \left((\omega_{i,e} - \omega_{i,w}) + \frac{F(ncp)}{F_i(Soret)} (\omega_{i,w})(\tau_i) \right) \quad (4)$$

where $Nu_{m,i}$ includes effects of variable properties but not thermal diffusion or a mainstream turbulence, and F(ncp) is a correction factor for variable (non-constant) properties.

The most important term for the dew point temperature, plus the temperature dependence and magnitude of the vapor deposition rate is the "driving force" for species mass transport, i.e., the concentration gradient, $(\omega_{i,e} - \omega_{i,w})$, for each species contributing to the net deposition rate. At the boundary layer outer edge the trace species mass fractions, $\omega_{i,e}$, will depend on the kinetics and thermodynamics controlling the vapor phase composition. If local thermochemical equilibrium (LTCE) is achieved at station e near the stagnation line (point), then the species compositions $\omega_{i,e}$ are those corresponding to LTCE at the prevailing pressure, temperature, and overall elemental composition, the latter usually being close to the elemental compositions entering the combustor.

The situation is more subtle at the gas/condensate interface because, even if LTCE is imposed, the local element mass fractions of the inorganic con-

stituents will generally differ from those in the mainstream. Thermal diffusion and multicomponent diffusion both contribute to this element "segregation", hence self-consistent LTCE calculations at station w require simultaneous consideration of the transport laws and the LTCE condition. Thus, for the deposition of a single pure compound, say, $Na_2SO_4(c)$ below its "dew point", two constraints are simultaneously imposed:

(1) Vapor-Condensate Equilibrium (VCE): The vapor mixture composition at station w should be compatible with the thermochemical co-existence of $Na_2SO_4(c)$ at temperature T_w and pressure p.

(2) Trace Element Flux-Ratio: Because $Na_2SO_4(c)$ is being deposited, the molar fluxes of Na and S must stand in the ratio of 2:1 at the prevailing vapor compositions.

For mixed (multicomponent) condensates, the VCE constraint is based on equality of chemical potential of each chemical species i in both vapor and condensed phase, and trace element fluxes must stand in the same ratio as in the co-existing condensate.

The multicomponent chemically frozen boundary layer vapor deposition theory implies:

(1) Soret transport of high molecular weight vapors shifts the dew points in a given environment to a higher surface temperature than expected in the presence of Fick diffusion alone;

(2) In multicomponent systems with unequal diffusion coefficients, chemical element segregation at the VC-interface is also associated with a dew point shift when the LTCE-condition is imposed;

(3) The dew-point defined by extrapolating the CFBL-deposition rate to zero from below is different theoretically from that defined by the temperature at which a cooled surface will first exhibit surface condensation.

Thus, while vapor systems exhibit characteristic condensate onset conditions associated with the commonly accepted notion of a "dew point", this temperature is also influenced by transport and kinetic restrictions.

In contrast to previous treatments of vapor deposition (Refs. 76-82 and 83-84), the Rosner formulation (Refs. 76-82) or CFBL theory makes explicit provision in the sodium sulfate case for the effects of:

(1) Na-element transport via species of differing mobility (i.e., $NaCl(g)$, $NaOH(g)$, $Na(g)$, $Na_2SO_4(g)$, etc.);

(2) thermal (Soret) diffusion of heavy, Na-containing species;

(3) free stream turbulence intensity and scale.

Application of vapor diffusion CFBL deposition theory. - The CFBL theory has been applied to the prediction of deposition rates for sea salt-, sodium chloride-, and sodium sulfate-seeded burner rig experiments (Refs. 75, 77, and 79). While the comparison between theory and experiment is only encouraging, it must be recognized that burner rig experiments have not yet been developed to the point where there is adequate control of all variables involved.

A more definitive test of the accuracy of the CFBL theory has been made by Rosner, et al. (Refs. 80, 82, and 85) who use optical techniques to measure the deposition of B_2O_3 from BCl_3-seeded propane-air laboratory flat flames. The comparison of results shown in Fig. 4 indicate that for a precisely controlled experiment where conditions can be closely defined, the CFBL theory can be applied with confidence to predict deposition rates.

The results of the application of the CFBL theory to the sea salt-seeded burner rig deposition study are presented in Fig. 5. Agreement between the maximum deposition rates far below the dew point is reasonable but the predicted dependence on surface temperature exhibits plateau-like behavior not evident in this set of experimental results.

By examining the nature of the equilibrium calculated species concentrations in the combustion gas free stream and at the surface of the collector, some insight may be gained regarding the nature of the transporting species in the context of the CFBL theory. According to this model, $Na_2SO_4(c)$ growth on a surface occurs primarily via transport of $NaOH(g)$, $NaCl(g)$, and $Na(g)$, but not $Na_2SO_4(g)$. In fact, the $Na_2SO_4(g)$ species contributes to a net loss of the Na_2SO_4 condensate layer due to a negative concentration gradient for this species across the boundary layer. Thus, in the CFBL framework, gas phase conversion of NaCl to Na_2SO_4 in the available residence time is not necessary for the process of Na_2SO_4 deposition. Rather, of more importance are heterogeneous reactions at the gas/liquid interface which convert $NaCl(g)$, $NaOH(g)$, and $Na(g)$ in the presence of excess O_2 and S-containing vapor species to $Na_2SO_4(c)$. Of course, the mechanism of this conversion may involve an Na_2SO_4 molecule. This situation makes it clear that a multicomponent deposition theory is absolutely essential for engineering applications.

An interesting aspect of calculations of combustion gas and deposit compositions is consideration of what condensed phases, other than Na_2SO_4, might be expected to deposit from sodium-seeded combustion gases. Na_2SO_4 was the only condensate expected over a wide range of temperatures for an equivalence ratio of less than one (i.e., oxidizing conditions). Under the conditions investigated, the calculations predict that no NaCl or NaOH condensates form. Even if $Na_2SO_4(c)$ were prohibited from forming (by omitting data for this phase from the program library) no NaCl or NaOH condensates would form. The calculations show that the phase that would likely form, from a thermodynamic viewpoint, would be Na_2CO_3. The high stability of the HCl molecule is also important here. This phenomenon illustrates that even though a molecule with a certain stoichiometry (such as NaCl) is one of the more stable gases in a complex equilibrium, the same composition may not be the most stable condensed phase. Indeed, the deposition of Na_2CO_3 has been observed from Na-seeded, sulfur-free propane/air flames (Ref. 41). Thus, it is not surprising that, in practice, NaCl is rarely detected as a condensed phase deposit in turbine engines or burner rigs. Situations in which NaCl deposits were observed (Refs. 39, 42, and 86), at levels greater than those predicted by Raoult's Law (Ref. 88), are likely attributable to particle capture.

Another application of the CFBL vapor diffusion deposition rate theory has been made by Helt (Ref. 89). He used the theoretical framework to calculate dew points and deposition rate for sodium sulfate formation in the flue gas of a coal-fired pressurized fluidized bed combustor. Helt's calculations are presented in clear, step-by-step detail and provide an excellent procedural guide for making the numerous involved calculations.

Particle diffusion contribution. - As Table II indicates, the diffusive modes of mass transport considered above for vapors only represent one extreme in the deposition behavior of molecules and particles. At the opposite extreme are particles so large that they cannot follow the motion of the carrier gas, i.e., inertial effects dominate. Between the extremes lies a large range of particle sizes where thermophoresis can dominate the rate of deposition to cooled surfaces. Considerable effort is being devoted to understanding deposition rate behavior in this region (Refs. 76, 79, 81 and 90-94).

As is well known, the capture efficiency of aerosol particles in iso-thermal forced convection systems falls off with increased particle size, reaching a minimum value (perhaps of the order of only 10^{-3} - 10^{-4} percent) before the onset of inertial deposition. Rosner found that this minimum

11

capture rate can be dramatically altered (e.g., over two decades) by thermophoretic particle transport to cooled (from heated) surfaces (Refs. 95-97). The above mentioned theoretical framework for dealing with the simultaneous effects of Brownian and thermophoretic transport can be used to illustrate this effect. For example, consider the capture of a $Na_2SO_4(1)$ droplet from a combustion gas flow over cooled targets simulating gas turbine engine blades. Figure 6 shows anticipated capture efficiency, for sodium sulfate transport to a cooled cylinder in crossflow, plotted as a function of particle diameter for three surface temperatures. Note the almost two decade augmentation in deposition rate predicted for cold collector surfaces at particle sizes just below the onset of "pure" inertial impaction. In terms of the CFBL theory applied to small particles, the effect of particle thermophoresis is governed by the dimensionless thermophoretic "suction" parameter which can attain large values in the particle size range of interest, even if negligible for clusters of molecular dimensions. Other examples of the importance of thermophoresis in the capture of intermediate size particles are included in the literature (Refs. 95-98).

The combined effects of diffusion and inertia are the subject of very recent research (Refs. 97 and 98). This work will permit understanding of the gradual transition that actually occurs between the diffusional and inertial branches shown in Fig. 6. Whereas "pure" inertial deposition theory leads one to expect the existence of a critical particle size above which inertial impaction becomes possible, the recent results show that the capture of particles below this size are also influenced by inertia. This effect manifests itself in inertially produced changes in the local mass loading of particles (i.e., inertial enhancement or centrifugal depletion). Once the inertially influenced distribution of local particle mass loading is achieved at the outer edge of the Brownian diffusion sublayer, SFBL theory yields the corresponding distribution of the diffusional deposition-rate. Necessary further research is in progress to deal with the important case of particles which are too large to follow the turbulent eddy motion within the velocity and thermal boundary layers.

CONCLUDING REMARKS

High pressure mass spectrometric flame sampling techniques have been used to help elucidate the flame chemistry of some sodium-sulfur and potassium-sulfu.-seeded laboratory flame systems. Condensible high temperature molecular species have been directly identified and some of the kinetics regarding the time for their formation has been established. Measured compositions of the gaseous flame products, for these seeded flames, have been shown to agree with those predicted by equilibrium thermodynamic calculations. The gas phase chemistry for the sodium-sulfur-seeded flames has been related to deposition processes and high temperature corrosion.

Deposition measurements, made for numerous combustion systems containing a wide variety of fuel and air impurities, have been instrumental in contributing to understanding of the mechanisms of deposition. These measurements have also established the predominant role played by vapor diffusion in the deposition of corrosive agents like sodium sulfate. Vapor diffusion deposition rate theories have evolved to the point where they now include the effects of multicomponent composition, thermal diffusion, variable gas properties across the gaseous boundary layer and free stream turbulence. Progress is also being made in efforts to include particle size effects in deposition theories and some important insights have already emerged.

Without question, significant advances have recently been made in understanding environmental attack aspects of pertinent combustion and deposition phenomena. However, increased understanding has also heightened awareness that there is need for additional specific research. Some of the most pressing needs are:

(1) Direct measurement of the gaseous and particulate composition of real combustion systems' product effluent.

(2) Modeling of the kinetics of metal-containing hydrocarbon flames.

(3) Phase equilibrium data and computer models of multielement, vapor/liquid and vapor/solid equilibrium as required for application to solution condensate deposition rate theory.

(4) Direct measurements of transport properties of inorganic vapor molecules.

(5) Development of a transport theory to account for effects of boundary layer condensation on deposition rate.

REFERENCES

1. Comparative Evaluation of Phase I Results from the Energy Conversion Alternatives Study (ECAS). NASA TM X-71855, 1976.

2. Evaluation of Phase 2 Conceptual Designs and Implementation Assessment Resulting from the Energy Conversion Alternatives Study (ECAS). NASA TM X-73515, 1977.

3. Grisaffe, S. J.; Lowell, C. E.; and Stearns, C. A.: High Temperature Environmental Effects on Metals. Risk and Failure Analysis For Improved Performance and Reliability, J. J. Burke and V. Weiss, eds., Plenum Publishing Corp., 1980, pp. 225-242.

4. Mellor, A. M.; Leonard, P. A.; and Henderson, R. E.: Turbopropulsion Combustion Research Needs. ASME Paper 80-GT-164, Mar. 1980.

5. Freche, J. C.; and Ault, G. M.: Progress in Advanced High Temperature Turbine Materials, Coatings and Technology. NASA TM X-73628, 1977.

6. Lowell, C. E.; Grisaffe, S. J.; and Levine, S. R.: Toward More Environmentally Resistant Gas Turbines: Progess in NASA Lewis Programs. NASA TM X-73499, 1976.

7. Barrett, C. A.; Johnston, J. R.; and Sanders, W. A.: Static and Dynamic Cyclic Oxidation of 12 Nickel-, Cobalt-, and Iron-Base High-Temperature Alloys. Oxid. Met., vol. 12, no. 4, 1978, pp. 343-377.

8. Barrett, C. A.; and Lowell, C. E.: Comparison of Isothermal and Cyclic Oxidation Behavior of Twenty-Five Commercial Sheet Alloys at 1150° C. Oxid. Met., vol. 9, no. 4, 1975, pp. 307-355.

9. Lowell, C. E.; and Deadmore, D. L.: The Role of Thermal Shock in Cyclic Oxidation. NASA TM-78876, 1978.

10. Wasielewski, G. E.; and Rapp, R. A.: High Temperature Oxidation. The Superalloys, C. T. Sims and W. C. Hagel eds., John Wiley and Sons, 1972, pp. 287-316.

11. Barrett, C. A.: 10,000-Hour Cyclic Oxidation Behavior at 815° C (1500° F) of 33 High-Temperature Alloys. Proceedings of Conference on Environmental Degradation of Engineering Materials, M. R. Louthan and R. P. McNitt, eds., United States National Science Foundation and Virginia Polytechnic Institute and State University, 1977, pp. 319-327.

12. Wright, I. G.: Oxidation of Iron-,Nickel-, and Cobalt-Base Alloys. MCIC-72-07, Battelle Columbus Labs., 1972. (AD-745473)

13. Reid, W. T.: External Corrosion and Deposits: Boilers and Gas Turbines; American Elsevier Pub. Co. Inc., 1971.

14. Bryers, R. W., ed.: Ash Deposits and Corrosion Due to Impurities in Combustion Gases. Hemisphere Publishing Corp., 1978.

15. Hart, A. B.; and Cutler, A. J. B.: Deposition and Corrosion in Gas Turbines. John Wiley and Sons, Inc., 1973.

16. Lowell, C. E.; Sidik, S. M.; and Deadmore, D. L.: Effect of Sodium, Potassium, Magnesium, Calcium and Chlorine on the High Temperature Corrosion of IN-100, U-700, IN-792 and Mar M-509. NASA TM-79309, DOE/NASA/2593-79/12, 1980.

17. Deadmore, D. L.; Lowell, C. E.; and Kohl, F. J.: The Effect of Fuel-to-Air Ratio on Burner-Rig Hot Corrosion. NASA TM-78960, 1978.

18. Bornstein, N. S.; Decrescente, M. A.; and Roth, H. A.: Effect of Vanadium and Sodium Compounds on Accelerated Oxidation of Nickel-Base Alloys. UARL-L910983-4, United Aircraft Corp., 1972. (AD-745292)

19. Miller, R. A.: Analysis of the Response of a Thermal Barrier Coating to Sodium- and Vanadium-Doped Combustion Gases. NASA TM-79205, DOE/NASA/2593-79/7, 1979.

20. Zetlmeisl, M. J.; May, W. R.; and Annand, R. R.: High Temperature Corrosion in Gas Turbines and Steam Boilers by Fuel Impurities; Part V-Lead Containing Slags. ASME Paper 74-WA/CD-4, Nov. 1974.

21. Wright, I. G.; Price, C. W.; and Herclenroeder, R. B.: State of the Art and Science Report on Design of Alloys Resistant to High Temperature Erosion/Corrosion in Coal Conversion Environments. EPRI-FP-557, Electric Power Research Institute, 1978.

22. Barkalow, R. H.; and Pettit, F. S.: Erosion/Fouling Effect of Fly Ash in High Velocity Combustion Gases. PWA-79-200-7072, Pratt and Whitney Aircraft, 1979. (EPRI Contract No. RP 979-4).

23. Jaffee, R. I.; and Stringer, J.: High-Temperature Oxidation and Corrosion of Superalloys in a Gas Turbine. High Temp.-High Pressures, vol. 3, no. 2, 1971, pp. 121-135.

24. Stringer, J.: Hot Corrosion of High-Temperature Alloys. Annual Review of Materials Science, Vol. 7, R. A. Huggins, R. H. Bube and R. W. Roberts, eds., Annual Reviews, Inc., 1977, pp. 477-509.

25. Stringer, J.: Hot Corrosion in Gas Turbines. MCIC-72-08, Battelee Columbus Labs., 1972.

26. Hot Corrosion in Gas Turbines - Mechanisms, Alloy and Coating Development, Environmental Effects, and Evaluation. NMAB-260, National Materials Advisory Board, 1970. (AD-870745.)

27. Santoro, G. J.: Hot Corrosion of Four Superalloys - HA-188, S-57, IN-617, and TD-NiCrAl. Oxid. Met., vol. 13, no. 5, 1979, pp. 405-435.

28. Santoro, G. J.: Hot Corrosion of Co-25Cr-10Ni-5Ta-3Al-0.5Y Alloy/S-57/. Corros. Sci., vol. 18, 1978, pp. 651-677.

29. Santoro, G. J.; and Barrett, C. A.: Hot Corrosion Resistance of Nickel-Chromium-Aluminum Alloys. J. Electrochem. Soc., vol. 125, no. 2, 1978, pp. 271-278.

30. Hodge, P. E.; et al.: Thermal Barrier Coatings: Burner Rig Hot Corrosion Test Results. NASA TM-79005, DOE/NASA/2593-78/3, 1978.

31. Deadmore, D. L.; and Lowell, C. E.: Effects of Impurities in Coal-Derived Liquids on Accelerated Hot Corrosion of Superalloys, NASA TM-81384, DOE/NASA/2593-79/13, 1980.

32. Wilson, J. S.; and Redifer, M. W.: Equilibrium Composition of Simulated Coal Combustion Products: Relationship to Fireside Corrosion and Ash Fouling. J. Eng. Power, vol. 96, no. 2, Apr. 1974, pp. 145-152. (Also ASME Paper 73 WA/CD-6, Nov. 1973.)

33. Cutler, A. J. B.; et al.: The Role of Chloride in the Corrosion Caused by Flue Gases and Their Deposits. J. Eng. Power, vol. 93, no. 3, July 1971, pp. 307-312. (Also ASME Paper 70-WA/CD-1, Nov. 1970.)

34. Goldberg, S. A.; Gallagher, J. J.; and Orning, A. A.: A Laboratory Study of High-Temperature Corrosion on Fireside Surfaces of Coal-Fired Steam Generators. J. Eng. Power, vol. 89, no. 2, Apr. 1968, pp. 193-198. (Also ASME Paper 67 WA/CD-2, Nov. 1967.)

35. High Temperature Gas Turbine Engine Component Materials Testing Program: Task I, Fireside I, Final Report. FE-1765-44, Dept. of Energy, 1978.

36. Deadmore, D. L.; and Lowell, C. E.: Airfoil Cooling Hole Plugging by Combustion Gas Impurities of the Type Found in Coal Derived Fuels. NASA TM-79076, DOE/NASA/2593-79/1, 1979.

37. Deadmore, D. L.; and Lowell, C. E.: Plugging of Cooling Holes in Film-Cooled Turbine Vanes. NASA TM X-73661, 1977.

38. Nealy, D. A.; Timmerman, W. H.; and Cohn, A.: Investigation of the Influence of Contaminated Fuel on Turbine Vane Surface Deposition. AIAA Paper 80-1113, June 1980.

39. Jackson, P. J.; and Duffin, H. C.: Deposition of Alkali-Metal Salts from Flue Gas. The Mechanism of Corrosion by Fuel Impurities, Proceedings of the International Conference, H. R. Johnson and D. J. Littler, eds., Butterworths (London), 1963, pp. 427-442.

40. Hanby, V. I.: Sodium Sulfate Formation and Deposition in Marine Gas Turbines. Eng. Power, vol. 96, no. 2, Apr. 1974, pp. 129-133. (Also ASME Paper 73-WA/CD-2, Nov. 1973.)

41. Durie, R. A.; Milne, J. W.; and Smith, M. Y.: The Deposition of Salts from Hydrocarbon Flames Containing Sodium and Sulphur Species. Combust. Flame, vol. 30, no. 3, 1977, pp. 221-230.

42. Dunderdale, J.; and Durie, R. A.: Some Aspects of the Behavior of Sodium Salts in Flames. Inst. Fuel, J., vol. 37, no. 286, 1964, pp. 493-500.

43. Santoro, G. J., et al.: Deposition and Material Response from Mach 0.3 Burner Rig Combustion of SRC-11 Fuels. NASA TM-81634, DOE/NASA/2593-20, 1980.

44. Santoro, G. J.; Calfo, F. D.; and Kohl, F. J.: Material Response From Mach 0.3 Burner Rig Combustion of a Coal-Oil Mixture. NASA TM-81686, DOE/NASA/2593-81, 1981.

45. Fristrom, R. M.; and Westenberg, A. A.: Flame Structure. McGraw-Hill Book Co., 1965.

46. Gaydon, A. G.; and Wolfhard, H. G.: Flames: Their Structure, Radiation and Temperature. Chapman and Hall Ltd (London), Third ed., 1970.

47. Hastie, J. W., High Temperature Vapors: Applications in Materials Science and Technology. Academic Press, 1975. (and references cited therein).

48. Kaskan, W. E.: The Reaction of Alkali Atoms in Lean Flames. Symposium International on Combustion, 10th, The Combustion Institute, 1965, pp. 41-46.

49. Jensen, D. E.; and Jones, G. A.: Alkaline Earth Flame Chemistry. Proc. Roy. Soc. (London), Series A, vol. 364, no. 1719, Dec. 1978, pp. 509-535, and reference cited therein.

50. Hedley, A. B.; and Papavergos, P.: An Investigation of Acid Smut Formation in an Industrial Boiler Plant. Ash Deposits and Corrosion Due to Impurities in Combustion Gases, R. W. Bryers, ed., Hemisphere Publishing Corp., 1978, pp. 113-128.

51. Glassman, I.: Combustion. Academic Press, 1977, pp. 228-240.

52. Reid, W. T.: Corrosion and Deposits in Combustion Systems. Combustion Technology: Some Modern Developments, H. B. Palmer and J. M. Beer, eds., Academic Press, 1974, pp. 35-59.

53. Muller, C. H.; et al.: Sulfur Chemistry in Flames. Seventeenth Symposium International on Combustion, The Combustion Institute, 1979, pp. 867-879.

54. Cullis, C. F.; and Mulcahy, M. F. R.: The Kinetics of Combustion of Gaseous Sulphur Compounds. Combust. Flame, vol. 18, no. 2, 1972, pp. 225-292.

55. Hedley, A. B.: A Kinetic Study of Sulfur Trioxide Formation in a Pilot Scale Furnace. The Mechanism of Corrosion by Fuel Impurities, H. R. Johnson and D. J. Littler, eds., Butterworths (London), 1963, pp. 204-215.

56. Fenimore, C. P.: Two Modes of Interaction of NaOH and SO_2 in Gases From Fuel-Lean H_2-Air Flames. Fourteenth Symposium International on Combustion, The Combustion Institute, 1973, pp. 955-963.

57. Durie, R. A.; Johnson, G. M.; and Smith, M. Y.: Gas Phase Reactions of Sodium Species with Sulfur Species in Hydrocarbon Flames. Fifteenth Symposium International on Combustion, The Combustion Institute, 1975, pp. 1123-1133.

58. Kohl, F. J.; Stearns, C. A.; and Fryburg, G. C.: Sodium Sulfate: Vaporization Thermodynamics and Role in Corrosive Flames. Metal-Slag-Gas Reactions and Processes, Z. A. Foroulis and W. W. Smeltzer, eds., The Electrochemical Society, 1975, pp. 649-664. (Also NASA TM X-71641, 1975).

59. Stearns, C. A.; et al.: Investigation of the Formation of Gaseous Sodium Sulfate in a Doped Methane-Oxygen Flame. J. Electrochem. Soc., vol. 124, no. 7, July 1977, pp. 1145-1146. NASA TM X-73600, 1977.

60. Fryburg, G. C.; et al.: Formation of Sodium Sulfate and Potassium Sulfate in Flames Doped with Sulfur and Alkali Chlorides and Carbonates. High Temperature Metal Halide Chemistry, D. L. Hildenbrand and D. D. Cubicciotti, eds., The Electrochemical Society, Vol. 78-1, 1978, pp. 468-483. (Also NASA TM X-73794, 1977).

61. Stearns, C. A.; et al.: High Pressure Molecular Beam Mass Spectrometric Sampling of High Temperature Molecules. Characterization of High Temperature Vapors and Gases, Materials Research Symposium, 10th, J. W. Hastie, ed., NBS Spec. Publ. 561/1, U.S. National Bureau of Standards, 1979, pp. 303-355. (Also NASA TM-73720, 1977).

62. Gordon, S.; and McBride, B. J.: Computer Program for Calculation of Complex Chemical Equilibrium Compositions Rocket Performance Incident and Reflected Shocks, and Chapman-Jouguet Detonations. NASA SP-273, 1971, Rev.

63. Biordi, J. C.; Lazzara, C. P.; and Papp, J. F.: Molecular Beam Mass Spectrometry Applied to Determining the Kinetics of Reactions in Flames. I - Empirical Characterization of Flame Perturbation by Molecular Beam Sampling Probes. Combust. Flame, vol. 23, Aug. 1974, pp. 73-82.

64. Steinberg, M.; and Schofield, K.: Laser Flourescence Studies of the Chemical Interactions of Sodium Species with Sulfur Bearing Fuels. (First and Second Semi-Annual Progress Rpts., Univ. of California; NASA Grant No. NSG-3256), Aug. 1979 and Mar. 1980.

65. Greene, F. T.; Beachey, J. E.; and Milne, T. A.: Direct Sampling and Characterization of Gaseous Species Responsible for Fireside Corrosion in Fossil Fuel-Fired Systems. FE-2288-19, U.S. Energy Research and Development Admin., 1977.

66. Greene, F. T.: Direct Sampling and Characterization of Gaseous Species Responsible for Fireside Corrosion in Fossil Fuel-Fired Systems. FE-2288-20, U.S. Energy Research and Development Admin., 1978.

67. Wilson, J. S.; and Gillmore, D. W.: Factors Influencing Formation of Alkali Sulfates in Fossil Fuel Combustion, MERC/RI/77-5, U.S. Dept. of Energy, 1977.

68. Hedley, A. B.; Brown, T. D.; and Shuttleworth, A.: Available Mechanisms for Deposition From a Combustion Gas Stream. ASME Paper 65 WA/CD-4, Nov. 1965.

69. Hedley, A. B.; Brown, T. D.; and Shuttleworth, A.: Vanadium Pentoxide Deposition from Combustion Gases. J. Eng. Power, vol. 88, no. 2, Apr. 1966, pp. 173-178.

70. Brown, T. D.: Deposition of Sodium Sulphate from Combustion Gases. J. Inst. Fuel, vol. 39, no. 38, 1966, pp. 378-385.

71. Stearns, C. A.; Kohl, F. J.; and Fryburg, G. C.: The Chemistry of Sodium Chloride Involvement in Processes Related to Hot Corrosion. Advanced Materials for Alternative Fuel Capable Directly Fired Heat Engines, J. W. Fairbanks and J. Stringer, eds., U.S. Dept. of Energy, CONF-790749, 1979, pp. 340-369.

72. Jackson, P. J.: Deposition of Inorganic Material in Oil-Fired Boilers. Ash Deposits and Corrosion Due to Impurities in Combustion Gases, R. W. Bryers, eds., Hemisphere Publishing Corp., 1978, pp. 147-161.

73. Urbas, T. A.; and Tombinson, L. H.: Part 1: Formation and Removal of Residual Fuel Ash Deposits in Gas Turbines Formed at Firing Temperatures Below 982° C (1800° F). Ash Deposits and Corrosion Due to Impurities in Combustion Gases, R. W. Bryers, ed., Hemisphere Publishing Corp., 1978, pp. 309-320.

74. Hart, A. B.; et al.: Deposition of Sodium Compounds Under Gas Turbine Conditions. High Temperature Alloys for Gas Turbines, D. Coutsouradis, et al., eds., Applied Science Publishers Ltd. (London), 1978, pp. 81-107.

75. Kohl, F. J.; et al.: Theoretical and Experimental Studies of the Deposition of NA_2SO_4 from Seeded Combustion Gases. J. Electrochem. Soc., vol. 126, June 1979, pp. 1054-1061. (Also NASA TM X-73683, 1977).

76. Rosner, D. E.: Thermal (Soret) Diffusing Effects on Interfacial Mass Transport Rates. Physicochem. Hydrodyn., vol. 1, no. 2-3, 1980, pp. 159-185.

77. Rosner, D. E.; et al.: Chemically Frozen Multicomponent Boundary Layer Theory of Salt and/or Ash Deposition Rates from Combustion Gases. Combust. Sci. Technol., vol. 20, no. 3-4, 1979, pp. 87-106.

78. Srivastava, R.; and Rosner, D. E.: A New Approach to the Correlation of Boundary Layer Mass Transfer Rates with Thermal Diffusion and/or Variable Properties. Int. J. Heat Mass Transfer, vol. 22, Sep. 1979, pp. 1281-1294.

79. Rosner, D. E.; and Fernandez de la Mora, J.: Recent Advances in the Theory of Salt/Ash Deposition in Combustion Systems. Advanced Materials for Alternative Fuel Capable Directly Fired Heat Engines, J. W. Fairbanks and J. Stringer, eds., U.S. Dept. of Energy, CONF-790749, 1979, pp. 301-330.

80. Rosner, D. E.; et al.: Transport, Thermodynamic and Kinetic Aspects of Salt/Ash Deposition Rates from Combustion Gases. Characterization of High Temperature Vapors and Gases, Materials Research Symposium, 10th, J. W. Hastie, ed., NBS Spec. Publ. 561/2, U.S. National Bureau of Standards, 1979, pp. 1451-1476.

81. Rosner, D. E.; and Seshadri, K.: Experimental and Theoretical Studies of Laws Governing Salt/Ash/Soot Deposition from Combustion Gases. in Proc. Eighteenth Symposium International on Combustion, The Combustion Institute (in press).

82. Seshadri, K.; and Rosner, D. E.: J. Am. Inst. Chem. Eng. (in press).

83. McCreath, C. G.: The Fate of Sea Salt in a Marine Gas Turbine. Presented at the Conference on Gas Turbine Materials in a Marine Environment, Univeristy of Bath, England, Sep. 20-23, 1976, Session V, Paper 2.

84. Ross, K.: Condensation of Sulfuric Acid from Flue Gas on a Cooled Cylinder J. Inst. Fuel, vol. 38, no. 293, 1965, pp. 273-277.

85. Seshadri, K.; and Rosner, D. E.: Combust. Flame (in press).

86. Halstead, W. D.; and Raask, E.: Behavior of Sulfur and Chlorine Compounds in Pulverized Coal-Fired Boilers. J. Inst. Fuel, vol. 42, no. 344, 1969, pp. 344-349.

87. Bishop, R. J.; and Cliffe, K. K.: Condensation of Sodium Chloride Vapor from a Moving Gas Stream. J. Inst. Fuel, vol. 42, no. 342, 1969, pp. 283-285.

88. Stearns, C. A.; et al.: Interaction of Gas-Phase Sodium Chloride and Gas-Phase Hydrogen Chloride with Condensed Sodium Sulfate. High Temperature Metal Halide Chemistry, D. L. Hildenbrand and D. D. Cubicciotti, eds., The Electrochemical Society, Vol. 78-1, 1978, pp. 555-573. (Also NASA TM-73796, 1977.)

89. Helt, J. E.: Evaluation of Alkali Metal Sulfate Dew Point Measurement For Detection of Hot Corrosion Conditions in PFBC Flue Gas. ANL/CEN/FE-80-12, Argonne National Lab., 1980.

90. Fernandez de la Mora, J.: Deterministic and Diffusive Mass Transfer Mechanisms in the Capture of Vapors and Particles. PhD Dissertation, Yale University, 1980.

91. Rosner, D. E.; Israel, R.; and Zydney, A.: Effect of Thermophoresis on the Minimum Attainable Aerosol Diffusional Deposition Rate Before the Onset of Inertial Impactions. in Proceedings of the ACS/IEC-81 Symposium on Aerosol Systems, Jan. 26-28, 1981, Tuscon, Arizona (in press).

92. Talbot, L.; et al.: Thermophorisis of Particles in a Heated Boundary Layer. J. Fluid Mech. (in press).

93. Vermes, G.: Thermophoresis-Enhanced Deposition Rates in Combustion Turbine Passages. J. Eng. Power, vol. 101, no. 4, Oct. 1979, pp. 542-548.

94. Wenglarz, R. A.: An Assessment of Deposition in PFBC Power Plant Turbines. ASME Paper 80-WA/CD-1, Nov. 1980.

95. Rosner, D. E.: Mass Transfer from Combustion Gases. Presented at AIChE 73rd Annual Meeting 16-20 November 1980, Chicago, ILL. Submitted to J. Am. Inst. Chem. Eng.

96. Fernandez de la Mora, J.; and Rosner, D. E.: Proc. Third International Levich Conference, J. Physicochem. Hydrodyn. (in press).

97. Rosner, D. E.; and Fernandez de la Mora, J.: Inertial and Thermophoretic Effects on the Capture of Fuel Ash Particles by Gas Turbine Blades. Submitted to J. Eng. Power, 1981.

98. Rosner, D. E.; and Fernandez de la Mora, J.: Particle Transport Across Turbulent Non-Isothermal Boundary Layers. Submitted to J. Eng. Power, 1981.

TABLE I. - ALKALI METAL- AND SULFUR-CONTAINING COMPOUND ADDITIONS

TO METHANE-OXYGEN FLAMES

Flame system	Reactant gas composition (mole %)		Fuel/oxidant mass ratio	Calculated adiabatic flame temperature, K	Flame[a] speed, cm sec^{-1}
	Fuel	Oxidant			
$NaCl-SO_2$	8.9 CH_4 0.92 SO_2	84.1 O_2 5.9 H_2O 0.18 NaCl	0.072	2032	45
$NaCl-CH_3SH$	5.3 CH_4 1.0 CH_3SH	87.3 O_2 6.2 H_2O 0.19 NaCl	0.046	1678	43
$Na_2CO_3-SO_2$	9.3 CH_4 1.0 SO_2	83.6 O_2 6.0 H_2O 0.051 Na_2CO_3	0.077	2097	44
$KCl-SO_2$	9.3 CH_4 1.0 SO_2	83.5 O_2 6.0 H_2O 0.19 KCl	0.076	2088	44
$K_2CO_3-SO_2$	9.3 CH_4 0.92 SO_2	83.8 O_2 5.9 H_2O 0.025 K_2CO_3	0.075	2101	45

[a]The flame speed, V_o in cm sec^{-1}, was calculated on the basis of the STP flow velocity of the reactant gases.

TABLE II. - CHARACTERISTICS OF DEPOSITION FOR SPECTRUM OF PARTICE SIZES

Size range[a]	Mass transport mode	Deposition species	Transport mechanism	Deposition characteristics
1-10 Å	Vapor diffusion	Atoms and molecules (vapors)	Fick diffusion soret diffusion eddy diffusion	1. $T_{dp} < T_e$ 2. Low n and deposition on side away from line-of-sight 3. Low sensitivity to $T_e - T_w$ 4. Rate levels off for $T_w \ll T_{dp}$
10 Å-10^{-1} μm	Vapor diffusion transition	Heavy molecules (condensate aerosols, clusters, submicron particles)	Brownian diffusion eddy diffusion thermophoresis	1. $T_{dp} = T_e$ 2. Lowest n 3. High sensitivity to $T_e - T_w$ 4. Rate nearly linear with $T_e - T_w$
10^{-1}-100 μm	Inertial	Macroscopic particles	Inertial impaction eddy impaction	1. No apparent T_{dp} 2. Highest n 3. Independent of $T_e - T_w$ 4. Preferential deposition on side facing flow

[a]Mode of deposition is not fixed by particle size alone.
n = deposition or collection efficiency, T_{dp} = dew point temperature,
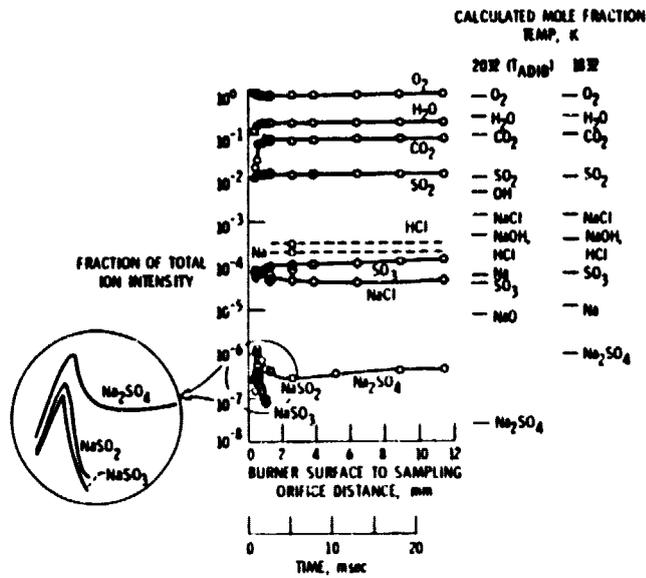T_e = gas mainstream temperature, T_w = wall temperature.

Figure 1. - Composition profiles for CH_4-O_2-H_2O-$NaCl$-SO_2 flame. Reactant composition in wt. % = CH_4, 4.7; O_2, 89.4; H_2O, 3.5; SO_2, 2.0; and $NaCl$, 0.35.
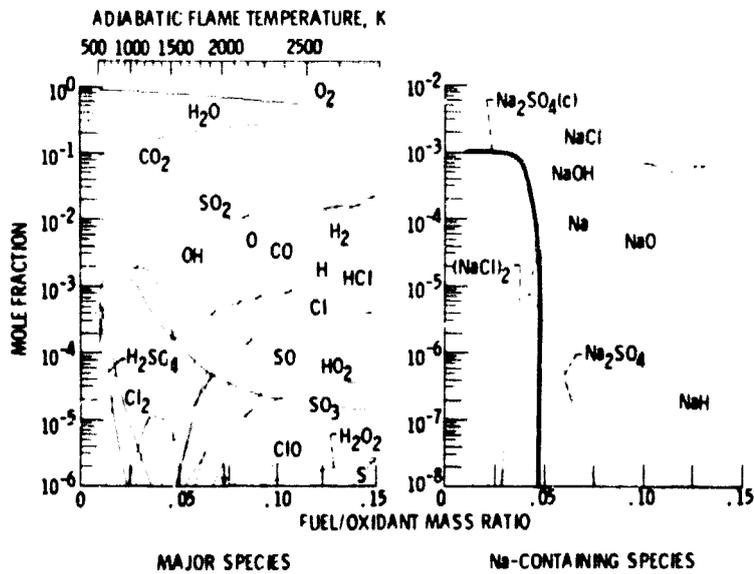

Figure 2. - Equilibrium chemical composition for $NaCl$-SO_2 doped methane-oxygen flame with fuel/oxidant mass ratio of 0.072. Reactant composition in wt. %: CH_4, 4.7; O_2, 89.4; H_2O, 3.5; SO_2, 2.0; and $NaCl$, 0.35.
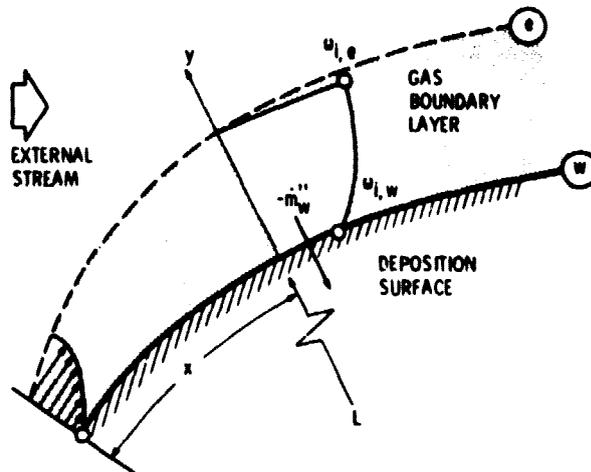
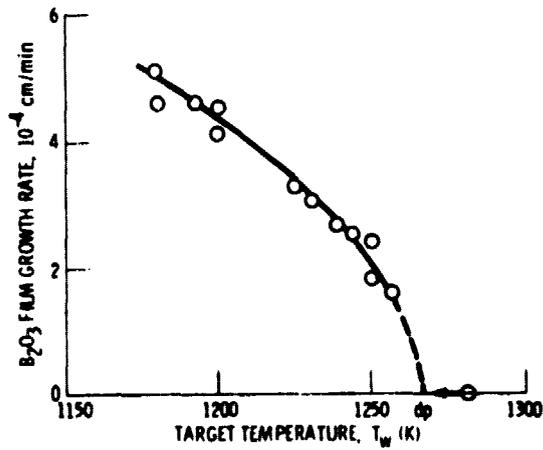Figure 3. - Schematic chemically frozen gaseous boundary layer on a cooled surface.

Figure 4. - Deposition rate of B_2O_3 from BCl_3-seeded propane-air frame, equivalence ratio - 1.70:10^{-2} (0.0812 moles BCl_3 per mole fuel). Deposit growth measured by optical interference technique (Ref. 82).
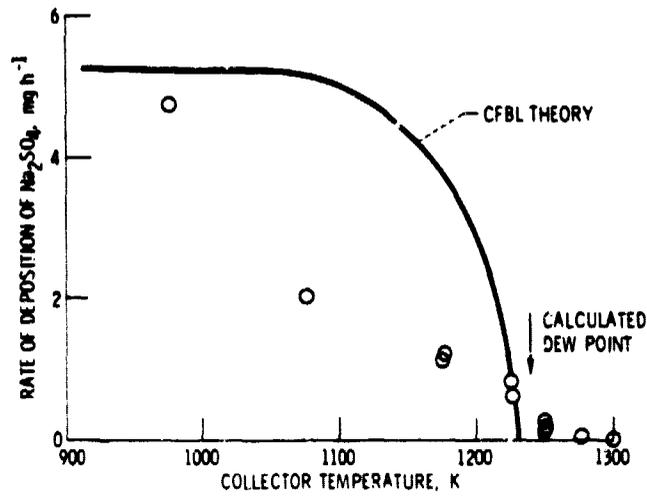
Figure 5. - Comparison of experimentally measured and theoreti-
cally calculated deposition rates of sodium sulfate on a cooled
platinum collector for a burner rig flame seeded with 11.3 wppm
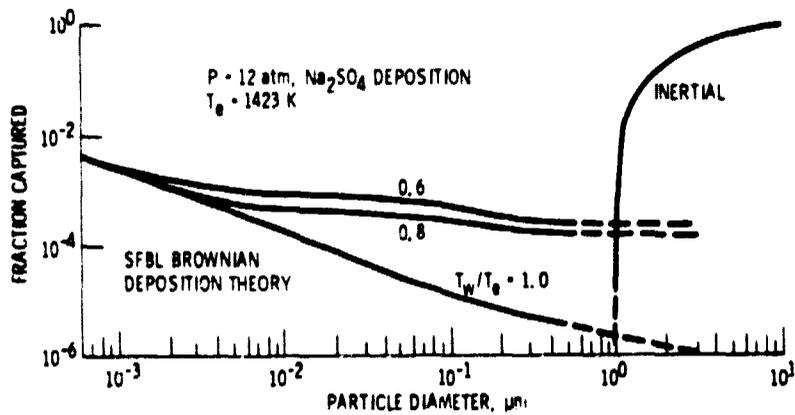sea salt and 0.038 wt. % sulfur in Jet A-1 fuel.

Figure 6. - SFBL theory predicted dependence of sodium sulfate deposition rate on
particle size.